

Vibrational and Thermal Evidence of Coordinated Water and Carboxylate Groups in Crystalline Calcium Malonate Dihydrate

E. V. Brusau, G. E. Narda, and J. C. Pedregosa

Area de Química General e Inorgánica "Dr. G. F. Puelles," Facultad de Química, Bioquímica y Farmacia, PID-CONICET 4929, Universidad Nacional de San Luis, Chacabuco y Pedernera, 5700 San Luis, Argentina

and

G. Echeverria and G. M. Punte

Profimo y Lanadi, Departamento de Física, Facultad de Ciencias Exactas, Universidad Nacional de La Plata, 1900 La Plata, Argentina

Received July 14, 1998; in revised form October 13, 1998; accepted October 21, 1998

Revision of the crystal structure of calcium malonate dihydrate, $[\text{Ca}(\text{mal})(\text{H}_2\text{O})_2]$, has shown that it belongs to the monoclinic system, space group $C2/m$, with $a = 13.857(6)$, $b = 6.8072(8)$, $c = 6.806(5)$ Å, $\beta = 106.31(7)^\circ$, $Z = 4$, and $V = 616.2(5)$ Å³. This is in agreement with one of the previous structural determinations, and nonequivalent water molecules and chelating and bridging carboxylate groups in the crystal lattice are evidenced. The infrared and Raman spectra were recorded and discussed in relation to the structural properties. Librational modes of water have been clearly identified and an assignment for all the internal modes is proposed. The thermal dehydration and decomposition processes were investigated using TG/DTA measurements. The structural model is consistent with the vibrational behavior and the two different temperatures observed in the dehydration process. © 1999 Academic Press

1. INTRODUCTION

The binding of the calcium ion to carboxylate and especially dicarboxylate ions has been the subject of several studies because of the importance of such interactions in the blood and bone proteins containing the modified amino acid residues γ -carboxylglutamic acid (Gla) and β -carboxyaspartic acid (Asa) (1–7). Einspahr and Bugg (8) have reported two binding ways for monocarboxylates: the monodentate mode and the bidentate one. In dicarboxylates there is an additional way of binding termed “malonate” since it is only available to a dicarboxylate like malonate.

Three hydrated forms of calcium malonate have been reported in the literature: $[\text{Ca}(\text{mal})(\text{H}_2\text{O})_2]$ involving mono- and bidentate (9–11) or monodentate and “malon-

ate” modes (12) and $[\text{Ca}(\text{mal})(\text{H}_2\text{O})_2] \cdot 2\text{H}_2\text{O}$ where malonate ions coordinate through mono- and bidentate interactions (13). Three previous crystallographic analyses of similar quality gave different descriptions of the monoclinic structure that includes the bidentate form (9–11). However, in one the noncentrosymmetric space group $C2$ was assumed (10), while in the other two (9, 11) it was found that space group $C2/m$ allows a better description of the crystal structure, in which Ca(II) is coordinated to eight O atoms, six belonging to four different malonate ions and two to the crystallographically inequivalent water molecules (W1 and W2). One of the carboxylate groups (CG1) binds three Ca(II) ions, while the other (CG2) is only bound to one. One of the water molecules (W1) is hydrogen bonded to two oxygen atoms belonging to CG2 carboxylate. The discrepancies between the centrosymmetric and noncentrosymmetric descriptions of the structure are mainly reflected in water molecules geometry and C–O bond lengths. In the noncentrosymmetric model only the W1 water molecule is involved in hydrogen bonds and all the C–O distances are dissimilar, the biggest variation being the C–O bond lengths of CG1. In the centrosymmetric approximation both water molecules are involved in hydrogen bonds; W2, which exhibits disorder, is hydrogen bonded to W1. The two determinations based on space group ($C2/m$) (9, 11) vary in unit-cell dimensions. This fact induces disparities in the Ca(II) coordination bond lengths and in W2 geometry.

In spite of the great effort devoted to the study of the title compound, no complete vibrational spectra interpretation (IR-Raman) was found in the literature, being O–H...O and C–H estimated IR frequencies only reported (12). Therefore, we have performed an IR and Raman analysis in order to study the interaction between Ca(II) and the donor

atoms of the dicarboxylate ion and the Ca–OH₂ bonds strength. As the understanding of the vibrational behavior is strongly dependent on the model employed, the crystal structure was revised doing new single crystal X-ray diffraction data. Thermogravimetry analysis (TGA) and differential thermal analysis (DTA) have been applied to verify the loss of two types of coordinated water (W1 and W2); the thermal study is complemented with information about decomposition of the anhydrous compound.

2. EXPERIMENTAL

Calcium malonate dihydrate was prepared by dissolving 2 mmol of Ca(NO₃)₂·4H₂O (Merck) in a 100-ml aqueous solution of malonic acid (0.02 M, Sigma) neutralized with NaOH to pH 7. The addition of the salt was made under stirring and heating conditions. The pH of the solution was 6.88 and it was left to cool at room temperature. Colorless and prismatic single crystals, suitable for X-ray diffraction studies were obtained after 1 week, then filtered, washed

with distilled water, and dried on P₄O₁₀. Anal Calcd for CaC₃H₆O₆: C, 20.24%; H, 3.37%; O, 53.88%; Ca, 22.51%. Found: C, 20.75%; H, 3.77%; O, 54.9%; Ca, 19.95%.

X-ray intensities were taken on an automatic four-circle CAD-4 diffractometer. For data collection and cell refinement the CAD-4 software (14) was used. The program MoLEN (15) was employed for data reduction. The structure was solved by direct methods using SHELXS86 (16) and refined by full matrix least-squares based on F^2 s using SHELXL93 (17). Structure analysis was performed with PLATON (18) and molecular graphics were done with ORTEP (19). All experimental details are shown in Table 1.

TG-DTA curves were obtained with a Shimadzu TGA-50H/DTA-50 thermal analyzer apparatus using flowing oxygen at 50 ml min⁻¹ in the temperature range of room temperature to 1000°C and at a heating rate of 10°C min⁻¹.

FTIR spectra were recorded on a Bruker IFS 66 spectrometer in the 4000–400 cm⁻¹ range, using the KBr pellet technique. For the expanded spectra at lower frequencies a Perkin Elmer 683 spectrometer was used. Spectral resolution

TABLE 1
Crystal Data and Structure Refinement for [Ca(mal)(H₂O)₂]

Crystal data and experimental details	
Chemical formula: C ₃ H ₆ CaO ₆	Crystal system: Monoclinic
$M_r = 178.16$	Space group: $C2/m$
a (Å) = 13.857(6)	α (°) = 90
b (Å) = 6.8072(8)	β (°) = 106.31(7)
c (Å) = 6.806(5)	γ (°) = 90
$Z = 4$	D_x (Mg m ⁻³) = 1.920
V (Å ³) = 616.2(5)	Crystal size: (approximately) 0.08 × 0.12 × 0.2 mm ³
$F(000) = 368.0$	No. of reflections for lattice parameters = 22
Radiation: MoK α	θ Range for lattice parameters (°) = 3 < 2 θ < 20
Wavelength (Å) = 0.71073	
Abs. coef. (mm ⁻¹) = 0.946	Temperature (K) = 295
Data collection	
Diffractometer type = CAD4	Collection method: ($\theta - 2\theta$)
Absorption correction type: SHELX76 (Sheldrick, 1976) Gaussian.	Absorption correction (T_{\min} , T_{\max}): 0.89 and 0.93
No. of refl. measured = 1200	$R_{\text{int}} = 0.0196$
No. of indep. refl. = 979	$\theta_{\text{max}} = 30$
No. of observed refl. = 979	No. of standard refl. = 1
Criterion for observed: $I > 3\sigma$	Max. variation of standards = 4%
$h_{\text{min}} = -19$	$h_{\text{max}} = 18$
$k_{\text{min}} = -1$	$k_{\text{max}} = 9$
$l_{\text{min}} = 0$	$l_{\text{max}} = 9$
Refinement	
Treatment of hydrogen atoms: the H's atoms were refined riding on bound C atoms.	Refinement on F^2
$R = 0.0355$	No. of refined parameters = 60
$R_w = 0.0987$	No. of reflections used in refinement = 979
$S = 1.104$	Weighting scheme $w = 1/[\sigma(F_o^2) + (0.00519P)^2 + (0.3667P)]$
	where $P = (F_o^2 + 2F_c^2)/3$
$(\Delta/\sigma)_{\text{max}} = 0.000$	$(\Delta\rho)_{\text{min}}$ (e Å ⁻³) = -0.626
Extinction correction method: none	$(\Delta\rho)_{\text{max}}$ (e Å ⁻³) = 0.617

Note. Source of atomic scattering factors. Ref. (38), Table 2.2B.

is better than 4 cm^{-1} in both cases. Raman spectrum was scanned on a Bruker IFS 66 Fourier Transform optical bench provided with the FRA 106 Raman accessory. Light of 1064 nm from Nd/YAG laser was used for excitation, the scattering geometry was 180° and 50 scans were usually accumulated with a resolution of 4 cm^{-1} .

3. RESULTS AND DISCUSSION

3.1. Crystal Structure

The comparison of our single crystal X-ray diffraction study with the others reported in the literature (9–11) shows that our results agree with those found by Briggman and Oskarsson (9); that is, the structure is centrosymmetric and the unit cell is the smallest of the reported ones. Crystal data are summarized in Table 1. The main features of the structure along with the label of the interacting groups are shown in Fig. 1. The observed discrepancies between bond lengths and angles of the carboxylate groups obtained in the present work and the corresponding values found with the other two structural models (10, 11) might be due to the existence of different degree of resonance involving these groups (see Fig. 1).

Both water molecules, with Ca(II)–O(W2) bond lengths shorter than the Ca(II)–O(W1) bond length are involved in hydrogen bonding (see Fig. 1). However, W2, which exhibits disorder, is only hydrogen bonded to W1, while W1 is hydrogen bonded to two oxygen atoms of CG2. These

interactions stabilize the carboxylate group by dissipating its negative charge. According to the above description and to the observed thermal ellipsoids of the water molecules it can be assumed that W1 is more tightly bound to the lattice than W2.

3.2. Vibrational Spectra

According to the general structural characteristics described above, it is evident that the internal vibrations of the title compound can be described by means of the following building units: carboxylate groups, methylene groups, and water molecules. The interpretation of its IR and Raman spectra is proposed from their comparison with those observed for malonic acid and related compounds found in the literature (20–22). Figure 2 shows the FTIR spectra of malonic acid and $[\text{Ca}(\text{mal})(\text{H}_2\text{O})_2]$, whereas the Raman spectrum of $[\text{Ca}(\text{mal})(\text{H}_2\text{O})_2]$ is shown in Fig. 3. The proposed assignment for these spectra is presented in Table 2. The analysis of the results confirms the structural data determined by XRD measurements.

Water modes. The presence of two kinds of crystallographically inequivalent water molecules in the lattice (W1 and W2) is evidenced by their IR characteristic vibrational modes. The frequency values are lower than those expected for free water stretching vibrations. This fact agrees not only with water coordination to the Ca(II)

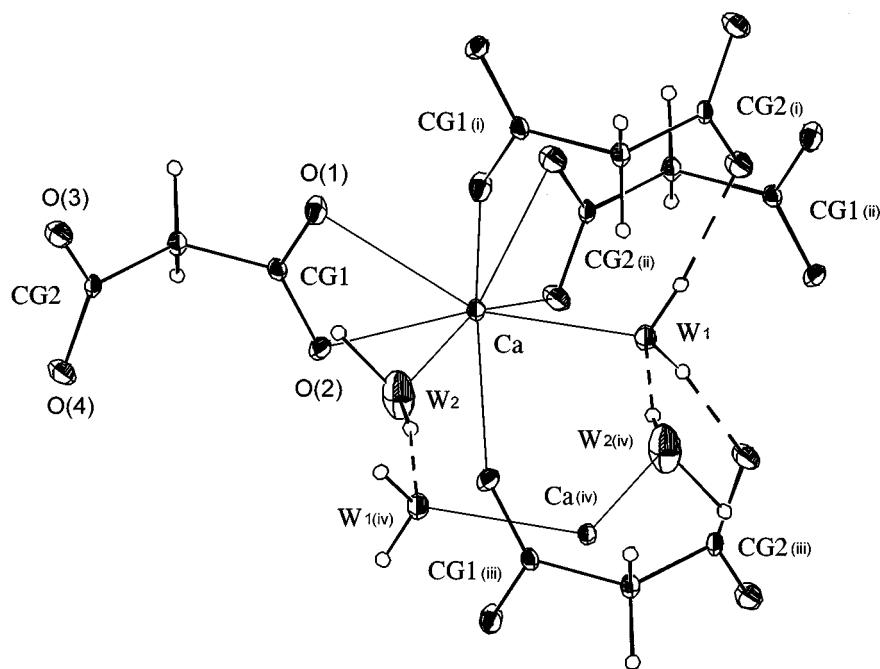


FIG. 1. View of the Ca(II) coordination and of the hydrogen bond system in the title compound. Thermal ellipsoids are drawn at 30% probability. Selected bond lengths (Å): Ca–O(1ⁱⁱⁱ, 2ⁱⁱ), 2.392(2); Ca–O(3, 4)ⁱⁱ, 2.529(2); Ca–OW1, 2.391(2); Ca–OW2, 2.371(3); C(1)–O(1, 2), 1.247(2); C(3)–O(3, 4), 1.253(2); C(1)–C(2), 1.529(4); C(2)–C(3), 1.527(4); OW1...O(3ⁱⁱⁱ, 4ⁱ), 2.724(2); OW2...OW1^{iv}, 2.843(4). Selected angles (°): OW1–H...O(3ⁱⁱⁱ, 4ⁱ), 171.69; OW2–H...OW1^{iv}, 172.3(4). Symmetry code: (i) $1/2 - x, 1/2 + y, -z$; (ii) $x, y, 1 + z$; (iii) $1/2 - x, -1/2 + y, -z$; and (iv) $-x, y, -z$.

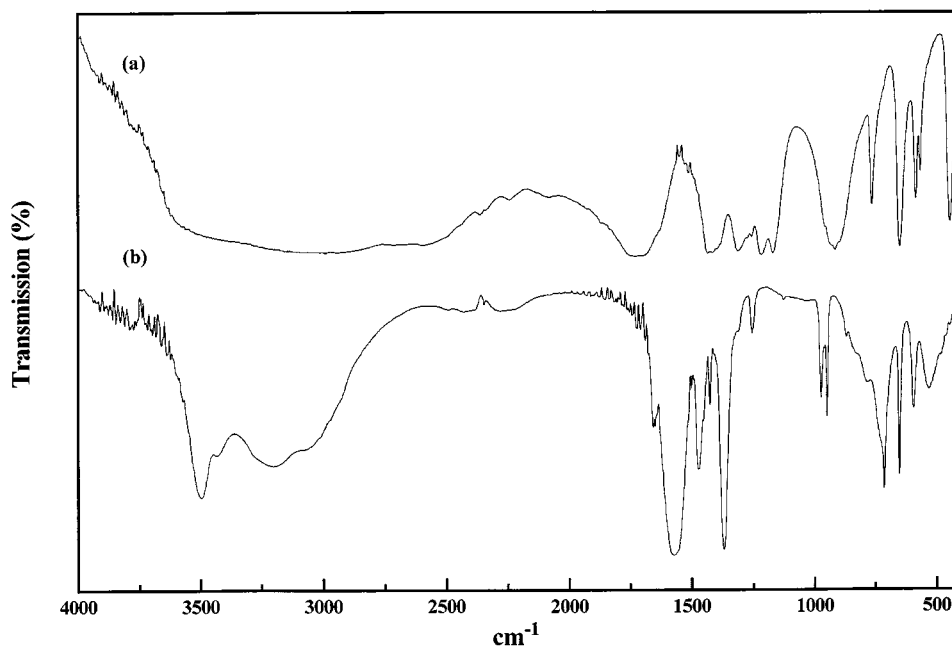


FIG. 2. FTIR spectra of (a) malonic acid and (b) $[\text{Ca}(\text{mal})(\text{H}_2\text{O})_2]$.

ion but also with the presence of hydrogen bonds in the lattice.

Two sets of bands at $3490\text{--}3430$ and $3200\text{--}3065\text{ cm}^{-1}$ appear in the OH stretching zone. The bands at the lower frequencies are attributed to W1 water molecules, which are hydrogen bonded to the CG2 group (see Fig. 1). The OH stretching modes of W2, which is only hydrogen bonded to W1,

correspond to the bands at the highest wavenumbers. This assignment is not only consistent with the structural model but also with the dehydration process reported in this paper.

The bending mode of H_2O appears as a doublet (1655 and 1650 cm^{-1}) due to the presence of different types of water molecules; these bands disappear after complete thermal dehydration.

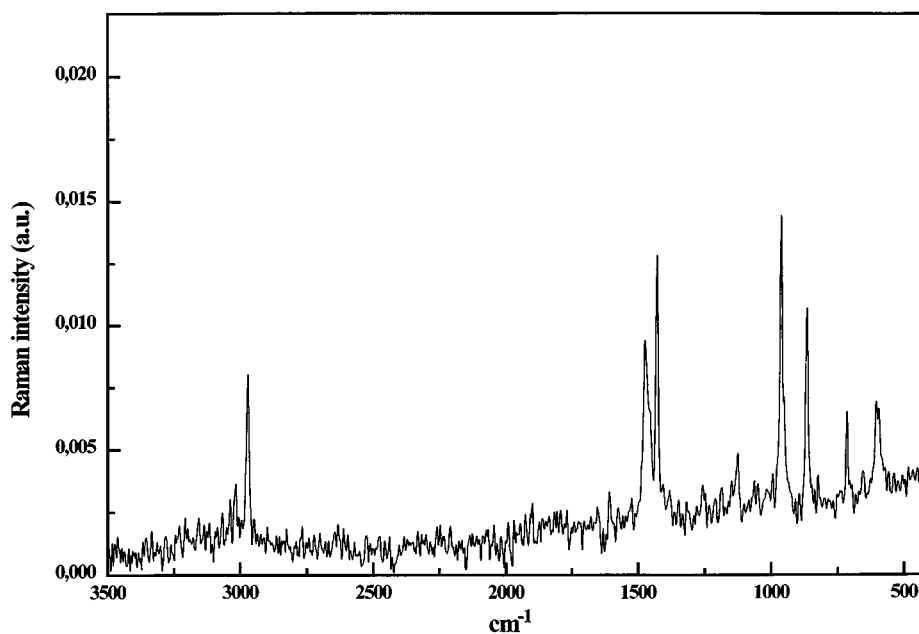


FIG. 3. Raman spectrum of $[\text{Ca}(\text{mal})(\text{H}_2\text{O})_2]$.

TABLE 2
Assignment of the Vibrational Spectra of $[\text{Ca}(\text{mal})(\text{H}_2\text{O})_2]$ (cm^{-1})

FTIR	Raman	Assignment
3490 (s)		$\nu_{\text{as}}(\text{OH})$ W2
3430 (sh)		$\nu_{\text{s}}(\text{OH})$ W2
3200 (br)		$\nu_{\text{as}}(\text{OH})$ W1
3065 (sh)		$\nu_{\text{s}}(\text{OH})$ W1
	2970 (s)	$\nu_{\text{s}}(\text{CH})$
2900*		$\nu_{\text{as}}(\text{CH})$
1655–1650 (m)(d)		$\delta(\text{H}_2\text{O})$
1565 (vs)(br)		$\nu_{\text{as}}(\text{OCO})$
1470 (s)	1470 (s)	$\delta(\text{CH}_2)$
1425 (m)		$\delta(\text{CH}_2)$
1365 (vs)	1430 (vs)	$\nu_{\text{s}}(\text{OCO})$
1255 (w)		$\rho_{\text{w}}(\text{CH}_2)$
1130 (vw)		$\nu_{\text{as}}(\text{CC})$
970 (m)	965 (vs)	$\nu_{\text{s}}(\text{CC})$
950 (m)		$\rho_{\text{r}}(\text{CH}_2)$
	870 (s)	$\delta(\text{CC})$
870 (vw)		$\rho_{\text{r}}(\text{H}_2\text{O})$
785 (w)		$\delta(\text{OCO})$
730* (sh)		$\rho_{\text{r}}(\text{H}_2\text{O})$
715 (s)	715 (m)	$\rho_{\text{w}}(\text{OCO})$
655 (s)		$\pi(\text{OCO})$
600 (m)	605 (m)	$\delta(\text{CCO})$
535 (m)		$\rho_{\text{w}}(\text{H}_2\text{O}) + \rho_{\text{t}}(\text{H}_2\text{O}) + \delta(\text{CCO})$
410 (w)		$\nu(\text{M-OH}_2)$

Note. ν_{as} , asymmetric stretching; ν_{s} , symmetric stretching; δ , deformation; ρ_{r} , rocking mode; ρ_{w} , wagging mode; ρ_{t} , twisting mode; π , out of plane deformation; s, strong; sh, shoulder; br, broad; *, overlap; m, medium; d, doublet; vs, very strong; w, weak; vw, very weak.

The librational modes of coordinated water, which usually present low intensity and are overlapped with other modes, are difficult to identify. The great diversity of frequency values assigned to these modes (23–25) are due to the significant influence of the crystal environment on them. Previous works dealing with metal malonate hydrates do not present a complete assignment of water vibrational modes, particularly for the librational ones (26, 27). Therefore, the present work adds to its knowledge. In order to make our assignment more reliable we have compared the IR spectra of $[\text{Ca}(\text{mal})(\text{H}_2\text{O})_2]$ with that of the product after complete thermal dehydration. Figure 4 shows them expanded in the region 900–400 cm^{-1} . The bands at 870, 730, 535, and 410 cm^{-1} disappear after the thermal procedure and therefore can be assigned to water modes. The two bands at the highest frequencies correspond to the rocking motion, whereas the band at 535 cm^{-1} is associated to wagging and twisting modes and the band at 410 cm^{-1} is attributed to M–OH₂ stretching vibration. The appearance of two bands for the rocking modes also supports the presence of two symmetrically inequivalent water molecules in the crystal (28). In the expanded IR spectrum, the M–OH₂ stretching mode has two components due to the different

bond strengths for Ca(II)–O(W2) and Ca(II)–O(W1) in accordance with the observed bond distances (see Fig. 1).

It is worth mentioning the marked effect of dehydration over the activation of some of the malonate ion vibrational modes, which are limited or overlapped in the initial compound. As can be seen in Fig. 4, the OCO bending (785 cm^{-1}) presents a strong activation while the band at 535 cm^{-1} is resolved in two well defined bands at 520 and 470 cm^{-1} , corresponding to CCO bending modes, when water molecules are lost.

OCO group modes. Malonic acid shows strong absorption bands at 1740 and 1710 cm^{-1} due to the carbonyl

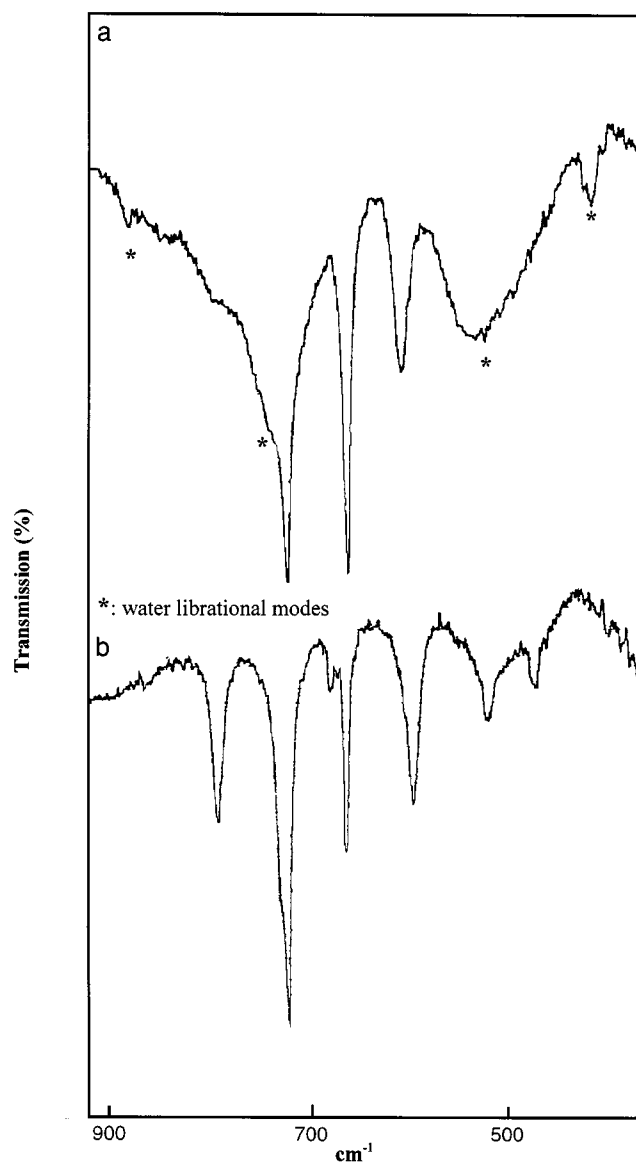


FIG. 4. The 900–400 cm^{-1} region IR spectra of (a) $[\text{Ca}(\text{mal})(\text{H}_2\text{O})_2]$ and (b) $[\text{Ca}(\text{mal})]$.

stretching vibration. This interaction effect is reduced in succinic acid and disappears for higher members of the series of dicarboxylic acids. For the free malonate ion, resonance is possible between the two C–O bonds; in consequence the characteristic carbonyl absorption is replaced by two bands between 1610 and 1550 cm^{-1} and between 1400 and 1300 cm^{-1} , which correspond, respectively, to the asymmetric and symmetric stretching vibration of the carboxylate structure. In general, each of these frequencies appears as a doublet, the separations being in the order of 20–40 cm^{-1} .

Our FTIR spectrum fits these general features very well. The carboxylate group asymmetric stretching vibration exhibits a broad band centered at 1565 cm^{-1} , which probably includes two components, and its symmetric stretching vibration appears at 1365 cm^{-1} without splitting. In the Raman spectrum, a strongly polarized line appears at 1430 cm^{-1} ; this line is characteristic of symmetric stretching vibration of the carboxylate group and it is clearly identified with this mode because its intensity is in accordance with the underlying theory which requires this mode to be strong in Raman. No evidence of carbonyl absorption is present, in agreement with the observed C–O distances (see Fig. 1).

According to our structural data, malonate ions interact with Ca(II) through chelating (CG2) or both chelating and bridging (CG1) carboxylate groups. Both carboxylate stretching modes are shifted to lower frequencies than the corresponding for the free malonate ion (e.g., sodium malonate) (26), indicating an increase in the coordination bond strength (29). In addition, the difference between the frequency values for both modes ($\Delta\nu$) is in the expected range for compounds having both chelating or chelating and bridging carboxylate groups, according to the criterion of Deacon and Phillips (30). The $\Delta\nu$ value is found to be higher

for compounds with an “ester-like” coordination mode, e.g., as for $\text{K}[\text{Al}(\text{mal})_2(\text{H}_2\text{O})_2] \cdot 2\text{H}_2\text{O}$ (31).

The deformation modes of carboxylate group are identified in IR at 785 cm^{-1} [$\delta(\text{OCO})$], 715 cm^{-1} [$\rho_w(\text{OCO})$], and 655 cm^{-1} [$\pi(\text{OCO})$]. The Raman spectrum shows a weak band at 715 cm^{-1} assigned to the [$\rho_w(\text{OCO})$] deformation mode.

CC modes. It is possible to observe a very weak band at 1130 cm^{-1} attributed to the $\nu_{\text{as}}(\text{CC})$ mode (32). The band at 970 cm^{-1} is identified with the $\nu_{\text{s}}(\text{CC})$ mode of the dicarboxylate group coincidentally with an intense Raman line at 965 cm^{-1} . This mode occurs with the expected intensity in IR and Raman spectra.

The intense band at 870 cm^{-1} in the Raman spectrum is assigned to the $\delta(\text{CC})$ mode.

CH₂ group modes. A sharp band at 2900 cm^{-1} in the IR spectrum of the dehydrated compound is assigned to the $\nu_{\text{as}}(\text{CH})$ mode. This band cannot be clearly observed in the spectrum shown in Fig. 2b because it is overlapped with the broad water absorption bands. Raman spectrum shows a line at 2970 cm^{-1} corresponding to the symmetric stretching mode.

At the 1400 cm^{-1} IR zone, two bands at 1470 and 1425 cm^{-1} are assigned to the bending modes of methylene consistent with a Raman line at 1470 cm^{-1} (33).

Wagging and rocking deformation modes are identified at 1255 and 950 cm^{-1} , respectively.

3.3. Thermal Behavior

The TG-DTA curves of calcium malonate dihydrate are shown in Fig. 5. Their examination indicates that all the transformations are associated with mass changes.

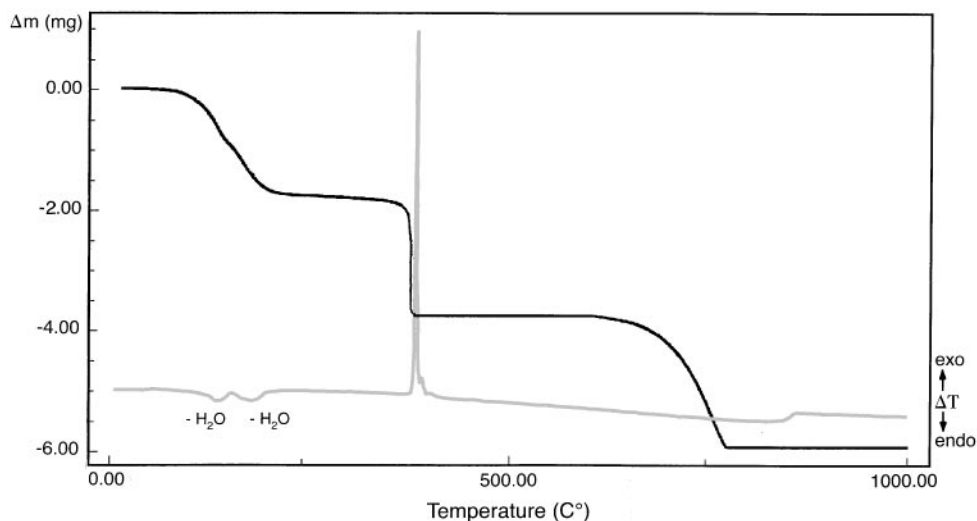


FIG. 5. TG-DTA curves of calcium malonate dihydrate.

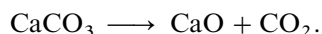
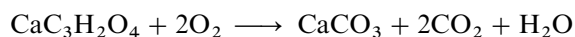
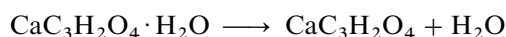
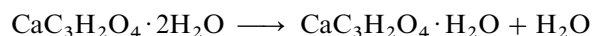
Appropriate combinations of X-ray powder diffraction and IR spectroscopy were used to characterize the final and intermediate products.

Dehydration proceeds via two stages; the first endothermic peak appears at 134°C and the second endothermic peak at 177°C. Each one corresponds to the loss of one water molecule yielding the anhydrous calcium malonate. The experimental weight loss in the TG curve is 20.69% (theoretical, 20.20%). These results are in accordance with the structural model. That is, one of the water molecules is more tightly bonded than the other. Therefore, it can be assumed that W2 is lost in the first stage of the dehydration process at 134°C, whereas W1 is lost at the higher temperature, 177°C.

The next stage is associated to the malonate ion decomposition resulting in calcium carbonate formation. The DTA curve shows a sharp exothermic peak at 365°C in coincidence with an experimental weight loss of 22.42% (theoretical, 23.42%). Several authors have considered the metal malonates decomposition process (34–37). Our results are in a close agreement with those reported by Muraishi *et al.* (37), our temperatures for dehydration and decomposition were higher and no elementary carbon was found in our products after each step.

On further heating the TG curve shows the last weight loss of 25.02% (theoretical, 25.01%). In DTA curve, an endothermic peak is observed at 772°C. This step corresponds to a calcium oxide formation from carbonate decomposition.

The thermal degradation process can be represented as follows:



4. CONCLUSIONS

This work reports an interpretation of the vibrational behavior (IR-Raman) of calcium malonate dihydrate. A reliable assignment for malonate and water modes, particularly the librational ones, has been done. The nature of water stretching modes region and the appearance of two bands for the bending and rocking modes indicate the existence of two symmetrically inequivalent water molecules in the crystal. The shifting of stretching modes to lower frequencies and bending modes to higher wavenumbers of water molecules confirms the presence of strong hydrogen bonds in the structure, whereas the vibrational features of malonate ion indicate the carboxylate groups as coordination sites involving mono- and bidentate modes.

Thermal procedures on the compound also allow us to confirm the presence of different types of water molecules.

Thus, vibrational and thermal information is in complete agreement with the structural model which supports the centrosymmetric description.

ACKNOWLEDGMENTS

This work was supported by CONICET and Universidad Nacional de San Luis. The authors are indebted to Dr. E. L. Varetti for help in the obtainment of Raman spectrum and to Dra. E. Ferrer for TG-DTA measurements. G. Echeverría is also with Facultad de Ingeniería, Universidad Nacional de La Plata.

REFERENCES

1. S. Magnusson, L. Sottrup-Jensen, T. E. Peterson, H. R. Morris, and A. Dell, *FEBS Lett.* **44**, 189 (1974).
2. J. Stenflo, P. Fernlund, W. Egan, and P. Roepstorff, *Proc. Natl. Acad. Sci. USA* **71**, 2730 (1974).
3. F. G. Prendergast and K. G. Mann, *J. Biol. Chem.* **252**, 840 (1977).
4. J. B. Lian, P. V. Hauschka, and P. M. Gallop, *Fed. Proc.* **37**, 2615 (1978).
5. M. R. Christy, R. M. Barkley, T. H. Koch, J. J. Van Buskirk, and W. M. Kirsch, *J. Am. Chem. Soc.* **103**, 3935 (1981).
6. A. Zell, H. Einspahr, and C. E. Bugg, *Biochemistry* **24**, 533 (1985).
7. M. E. Curry, D. S. Eggleston, and D. J. Hodgson, *J. Am. Chem. Soc.* **107**, 8234 (1985).
8. H. Einspahr and C. E. Bugg, *Acta Crystallogr. B* **37**, 1044 (1981).
9. B. Briggman and A. Oskarsson, *Acta Crystallogr. B* **33**, 1900 (1977).
10. A. Karipides, J. Ault, and A. T. Reed, *Inorg. Chem.* **16**, 3299 (1977).
11. R. E. Marsh and V. Schomaker, *Inorg. Chem.* **18**, 2331 (1979).
12. J. Albertsson, A. Oskarsson, and C. Svensson, *Acta Crystallogr. B* **34**, 2737 (1978).
13. D. J. Hodgson and R. O. Asplund, *Inorg. Chem.* **29**, 3612 (1990).
14. Enraf-Nonius CAD-4-PC, Version 1.2. Enraf-Nonius, Delft, The Netherlands, 1993.
15. C. K. Fair, MOLEN Version 1.0. Enraf-Nonius Structure Determination System. Enraf-Nonius, Delft, The Netherlands, 1990.
16. G. M. Sheldrick, SHELXS86, Program for the solution of crystal structures. Univ. of Göttingen, Germany, 1985.
17. G. M. Sheldrick, SHELXL93, Program for the refinement of crystal structures. Univ. of Göttingen, Germany, 1993.
18. A. L. Spek, *Acta Crystallogr. A* **46**, C34 (1990).
19. C. K. Johnson, ORTEPII. Report ORNL-5138. Oak Ridge National Laboratory, Tennessee, 1976.
20. L. J. Bellamy, "The IR Spectra of Complex Molecules," Vol. I. Chapman and Hall, London, 1975.
21. K. Nakamoto, "IR and Raman Spectra of Inorganic and Coordination Compounds," 5th ed. Wiley, New York, 1997.
22. J. T. Edsall, *J. Chem. Phys.* **5**, 508 (1937).
23. I. Gamo, *Bull. Chem. Soc. Jpn.* **34**, 760 (1961).
24. J. R. Ferraro and A. Walker, *J. Chem. Phys.* **42**, 1278 (1965).
25. I. Nakagawa and T. Shimanouchi, *Spectrochim. Acta A* **20**, 429 (1964).
26. M. J. Schmelz, I. Nakagawa, S. Mizushima, and J. V. Quagliano, *J. Am. Chem. Soc.* **81**, 287 (1959).
27. Y. Suzuki, *Thermochim. Acta* **255**, 155 (1995).
28. V. P. Mahadevan Pillai, V. U. Nayar, and V. B. Jordanovska, *J. Solid State Chem.* **133**, 407 (1997).
29. K. Nakamoto, Y. Morimoto, and A. E. Martell, *J. Am. Chem. Soc.* **83**, 4528 (1961).
30. J. B. Deacon and R. J. Phillips, *Coord. Chem. Rev.* **33**, 227 (1980).

31. A. Tapparo, S. Heath, P. Jordan, G. Moore, and A. Powell, *J. Chem. Soc. Dalton Trans.* 1601 (1996).
32. N. Gutmann, B. Müller, and H. Tiller, *J. Solid State Chem.* **119**, 331 (1995).
33. M. Kemiche, P. Becker, C. Carabatos-Nédelec, B. Wyncke, and F. Bréhat, *Vib. Spectrosc.* **11**, 135 (1996).
34. A. K. Galwey and M. A. Mohamed, *Solid State Ionics* **42**, 135 (1990).
35. Y. Suzuki, K. Muraishi, and H. Ito, *Thermochim. Acta* **258**, 231 (1995).
36. A. K. Galwey and M. A. Mohamed, *Thermochim. Acta* **273**, 239 (1996).
37. K. Muraishi, Y. Suzuki, and Y. Takahashi, *Thermochim. Acta* **286**, 187 (1996).
38. "International Tables for X-ray Crystallography," Vol. 4, Kluwer Academic, Norwell, MA, 1974.